# The Second-Generation Polysulfone Gas-Separation Membrane. I. The Use of Lewis Acid : Base Complexes as Transient Templates To Increase Free Volume

R. E. KESTING,* A. K. FRITZSCHE,† M. K. MURPHY, C. A. CRUSE, A. C. HANDERMANN, R. F. MALON, and M. D. MOORE,† *Permea, Inc., A Monsanto Company, 11444 Lackland Road, St. Louis, Missouri 63146*

## Synopsis

The second-generation polysulfone (PSU) gas-separation membrane is seen as a *trilayer* that is considerably more permeable and at least as selective as the first-generation bilayer that it has replaced. In air separation, a fourfold increase in oxygen permeability has been obtained with no loss in oxygen/nitrogen selectivity. The enhanced performance is the result of a membrane skin that is not only thinner, but also exhibits increased free volume and a graded density. *The key to the emergence of the trilayer morphology was the discovery of a hitherto unsuspected relationship between the size of solvent molecules within a sol and the free volume and permeability in the resultant gel!* Solvent molecules with a molar volume $V > \sim 147$ cc/mol function as transient templates (spacers) that decrease macromolecular packing density. As a practical matter, the low diffusivity (difficult extractibility) of large solvent molecules is circumvented by the use of 1 : 1 Lewis acid : base (A : B) complexes such as propionic acid : *N*-methyl pyrrolidone instead of neat solvents. Complexes whose acid and base strengths, respectively, lie between (Gutmann $47 < AN < 53$ and $27 < DN < 28$) are sufficiently stable to function as templates, while at the same time exhibiting the hydrolytic instability that leads to their ready disassociation and extraction by water. Selectivity is maintained by the use of A : B complexes whose Hildebrand solubility parameters differ from that of PSU by less than $\sim 1.3$ $(cal/cc)^{1/2}$. The emergence of the trilayer membrane is considered to be the second decoupling of permeability from selectivity. By the formation of an anisotropic (graded density) skin, permeability has been increased and selectivity maintained. This is analogous to the first decoupling by Loeb and Sourirajan who essentially replaced a thick dense monolayer film with a bilayer consisting of a thin skin of uniform density in series with a thick porous substructure.

## INTRODUCTION

The first-generation gas-separation membrane was based on polysulfone (PSU), a hydrophobic, high $T_g$, glassy polymer, because of its favorable separation characteristics and its outstanding chemical, mechanical, and thermal properties.[1] Integrally skinned asymmetric bilayers rather than dense film monolayers were employed because, as originally demonstrated by Loeb and Sourirajan,[2] the former are orders of magnitude more permeable, while retaining an almost equivalent selectivity. The skin of an integrally skinned asymmetric

* To whom correspondence should be sent: % Kesting Membrane Ventures, 3220 199th Ave. Ct.E., Sumner, WA 98390.

† Romicon Inc., Woburn, MA.

Journal of Applied Polymer Science, Vol. 40, 1557–1574 (1990)
 CCC 0021-8995/90/9-101557-18$04.00

bilayer is a film consisting ideally of a single layer of coalesced nodule aggregates.[3,4] In the case of the gelation of a sol of a hydrophilic polymer such as cellulose acetate, polymer-polymer interaction is only slightly greater than polymer-water interaction and the maintenance of a thin skin throughout and beyond the sol-gel transition is easily achieved. During the gelation of a sol of a hydrophobic polymer such as PSU, on the other hand, polymer-polymer and polymer-solvent interactions are considerably greater than is polymer-water interaction and the coalescence of more than a single layer of nodule aggregates may occur. This can result in skins that are both thicker and denser than those of membranes from hydrophilic polymers. Increased skin thickness and density, in turn, lead to greater resistance and lesser permeability than is the case where the skin consists of a single layer of less compacted nodule aggregates.

The problem of excessive coalescence of nodule aggregates in PSU membranes manifests itself macroscopically as shrinkage, that is, the diminuition of the width of a cast film or the diameter of a spun fiber during gelation and desolvation. This phenomenon is not unique to gas-separation membranes. It is encountered also during and after the formation of ultrafiltration membranes from the sulfone family of polymers and has received considerable attention in recent years.[5,6] Earlier workers employed inorganic acids during the various stages of membrane formation to retard shrinkage (Table I). They presumably reasoned that acids would neutralize basic solvents, thereby accelerating desolvation of the polymer and minimizing plasticization and densification. Cabasso et al. immersed already formed membranes into concentrated sulfuric acid in a postgelation step.[5] Tweddle et al. gelled membranes in an aqueous bath containing 25% $H_2SO_4$.[6] Tweddle et al. also exposed the cast solution to a mixture of HCl gas and air prior to gelation.[6] These treatments reduced shrinkage and significantly improved permeability with no loss in selectivity. A trend toward the use of inorganic acids at progressively earlier stages in membrane formation is apparent. The present study began as an attempt to abate shrinkage in PSU gas-separation membranes by the incorporation of inorganic acids into the sol, that is, into the earliest stage of membrane formation. It led ultimately to the invention and development of the second-generation PSU gas-separation membrane. This treatise is an introduction and overview whose principal objective is to explain the origin of the new trilayer structure and the relationship of the latter to membrane function. Additional reports of various aspects of this membrane will be published at a later date.

TABLE I
Use of Inorganic Acids for Shrinkage Control in Polysulfone Membranes

| Process step | | | | | |
|---|---|---|---|---|---|
| Sequence | Description | Acid | Membrane type | Reference | Date |
| 1 | Precasting (in sol) | $H_2SO_4$ | Gas separation | Present study | 1986 |
| 2 | Postcasting-pregelation | < 50% HCl gas | UF | 6 | 1983 |
| 3 | Gelation | 25% $H_2SO_4$ | UF | 6 | 1983 |
| 4 | Postgelation | Conc. $H_2SO_4$ | UF | 6 | 1975 |

## EXPERIMENTAL

### Fiber Spinning

Hollow fibers were prepared by a standard dry-wet spinning process. Filtered deaerated sol was spun from a tube-in-orifice-type spinnerette through an air gap and into an aqueous gelation bath. The system was maintained at a temperature sufficient to maintain adequate flow of the high-viscosity sols. Water was injected into the fiber lumen to maintain patency. The fiber was drawn at a rate of up to 100 m/min through water baths that were kept at or below room temperature. The fiber was wound onto a bobbin and washed with water for a time sufficient to quantitatively remove all of the components of the solvent vehicle. Hanks of fiber were then formed by skeining the fiber from the bobbin. These hanks were then hung vertically and dried rapidly at about 100°C.

### Gas-Permeability Testing

Gas-separation characteristics were obtained from 2.5 × 30 cm elements with a total active surface area of 0.4 $m^2$ and a packing factor of 50%. Each element contained about 1200 500 $\mu$m OD fibers. The elements were coated in a pervaporation mode from a solution consisting of 1% Sylgard in isopentane. Coated elements were placed in a pressure vessel, and oxygen and nitrogen permeabilities were measured at 50°C under 13.6 atm (200 psi) using a dry tank air feed. Surface permeance was calculated from the equation

$$P/l = \frac{QCF(14.7 \text{ psi/atm})}{n\pi t(76 \text{ cmHg/atm})(60 \text{ s/min})}$$

where $Q$ = the apparent gas flow reading from the mass flow meter [$cm^3$ (STP)/min], $CF$ = a conversion factor for the specific gas to change the apparent flux to the actual flux, $n$ = the number of fibers, $d$ = the outer diameter of the fiber (cm), $t$ = active fiber length, $P$ = the permeability through the fiber, and $l$ = skin thickness. The units for $P/l$ = gas-permeation unit GPU = $cm^3/cm^2$ s cm Hg ($\times 10^6$).

### Differential Scanning Calorimetry

Duplicate samples were tested on a DuPont Model 1090 DSC at a 20°C/min heating rate through and beyond the $T_g$ to 250°C. The $T_g$ obtained during the first excursion through the $T_g$ range was recorded as the first heat $T_g$, $T_g^*$. The latter is used as evidence for the existence of increased enthalpy and free volume in trilayer membranes.

### Oxygen Plasma Etching

The experimental details of the oxygen etching experiments (which support the existence of the graded density skin) are given elsewhere.[7]

### Infrared Spectra of Solvent Vehicles

IR spectra of pure and mixed solvent vehicles were recorded at room temperature on a Nicolet MX-I Fourier transform spectrometer. Sample liquids were examined as capillary films pressed between the surfaces of calcium fluoride optical flats and in some cases as dilute solution in cyclohexane using a 0.1 mm fixed path length cell with $CaF_2$ windows. Samples were examined under $N_2$ atmosphere, corrected for any residual atmospheric absorption, and analyzed digitally using Nicolet DX-I software programs. Resolution was better than 2 $cm^{-1}$.

### Acceptor and Donor Numbers

Acceptor number (AN) and donor number (DN) values are measures of the relative strength of Lewis acids and bases, respectively. They were either taken from the works of Gutmann et al.[8] and Mayer[9] or obtained by analagous experimental procedures.[7]

### Solubility Parameters

Hildebrand (total) solubility parameters ($\delta_t$) with units in $(cal/cc)^{1/2}$ were employed in this study. They were taken from the following sources: Barton[10]; BASF (2-chloropropionic acid $\delta_t$ = 12.4); AMOCO (Udel PSU $\delta_t$ = 10.55).

### Viscosimetry

Viscosimetric measurements were made with a Brookfield viscosimeter.

## RESULTS AND DISCUSSION

Although permeability results are often presented empirically and interpreted phenomenologically, we believe sufficient information is available to warrant the establishment of a physical model in light of which our gas-separation results may be interpreted. Because the new model also offers a plausible explanation for the origin of dual-mode sorption of gases, we refer to it as the intra- and internodular chain displacement/dual-mode model.[11]

### The Intra- and Internodular Chain Displacement/Dual-Mode Model

Sorption and permeability in glassy films and membranes is often interpreted in terms of the dual mode theory.[7,12,13] Two different populations of sorption sites are thought to exist: The smaller and more numerous correspond to the Henry's law mode of sorption; the larger are called Langmuir sorption sites. Whereas Henry's Law sites correspond to mean interchain displacements within the denser domains of the glassy polymer, the nature of the Langmuir sites remains obscure. Robertson,[14] for example, hypothesized that Langmuir sites are kinks in macromolecules that arise as a result of *cis-trans* isomerism. Pace and Datyner,[15] on the other hand, state that any such kinks serve only to increase average interchain displacement by a "smearing" process. Clearly, the relationship between structure and function in membrane gas separation re-

quires additional insight into membrane fine structure. Fortunately, more is known about this subject than many realize. This knowledge comes to us from the related field of reverse osmosis, which uses membranes whose structure has been intensively studied for the past three decades. Indeed, to be used in gas separation, an asymmetric reverse osmosis membrane need only be dried in such a manner that the structure that is present in its wet condition be maintained throughout and beyond the drying process. This can be achieved by both freeze-drying and solvent-exchange procedures.[16]

Reverse osmosis membranes are asymmetric bilayers consisting of thin "dense" (actually, finely porous) skins and thick low-resistance substructures that serve as mechanical supports for the skins. The skin is the functional part of the bilayer and determines both water permeability and salt retention (selectivity).[1,4,16] There are two species of skinned membrane: the integrally skinned asymmetric type in which skin and substructure layers are of the same material and are formed at more or less the same time by phase inversion, and the thin film composite wherein the two layers are formed separately, often from different materials.[4,16] The former is the sort originally developed by Loeb and Sourirajan[2] for reverse osmosis. It is also the kind almost exclusively employed in gas separation and will, therefore, be the sole object of our concern here.

There are several superimposed tiers of structure that are relevant to both dense films and integrally skinned asymmetric reverse osmosis and gas separation membranes.[11,17,18,20] Two that have been directly observed by electron microscopy are nodules and nodule aggregates. Nodules[11,17] were termed "spheres" by their discoverers Schultz and Asunmaa[18] and "primary particles" by Kamide and Manabe.[19] Each nodule is approximately 200 Å in diameter and contains several tens of individual macromolecules.[19] We believe that the disposition of the macromolecules within the nodule is a determining factor in gas separation.[11] It appears probable that the macromolecules are folded such that neighboring chain segments are parallel to one another over distances of at least 10 Å[11,15] and possibly over greater distances depending on chain stiffness. The displacements between the chains within the nodule are termed **intra**nodular chain displacements and are believed to be the domains where Henry's Law sorption prevails.[11] The relationship between nodules or primary particles and nodule aggregates on "secondary particles" was first explicitly stated by Kamide and Manabe.[19] Spherical nodules ($\sim$ 200 Å in diameter) agglomerate into larger (400–1000 Å in diameter) spherical nodule aggregates. These nodule aggregates were actually first seen by Panar et al.[3] who called them "micelles," a term, which although not explicitly mentioned in their paper, clearly implies aggregation of some sort. A reinvestigation of the electron micrographs of Panar et al.[3] by one of the present authors[11] revealed the presence of hemispherical proturbances, believed to be individual nodules, at the surface of the nodule aggregates. Panar et al.[3] showed that the skins of the integrally skinned asymmetric membrane consist of a single layer of what we now know to be coalesced and compacted nodule aggregates. However, although nodule aggregates can be seen in cross-sectional views of the membrane, they are not apparent in views of the top surface whereas the smaller nodules are. Therefore, the present authors agree with Schultz and Asunmaa,[18] who suggested that the gaps between

impinging nodules were the effective pores through which water permeates in reverse osmosis. However, these pores are not now considered to be free of matter. Rather, it is believed that these internodular spaces are simply regions of lower polymer density than that which is encountered within the nodule itself. Hence, internodular chain segments are farther apart than those within the nodule. It is, therefore, suggested that the *inter*nodular chain segment displacements represent the Langmuir sorption sites, whereas the *intra*nodular chain segment displacements, as already stated, represent the Henry's mode sites (Fig. 1). However, although we believe that intra and internodular chain displacements represent the two fundamental pore types in gas separation, other larger pores, which can be considered as defects, are also present. Panar et al.[3] showed that occasional gaps were found in the skin. These gaps represent regions where the coalescence of nodule aggregates is incomplete. They constitute the second type of pore found in reverse osmosis membranes. (The intranodular chain segment displacements are considered to be too small to be accessible to liquid water in reverse osmosis, although they are accessible to water vapor in gas separation.)

In any event, all such large pores must be sealed or otherwise eliminated before an asymmetric membrane can exhibit a selectivity to gas permeation

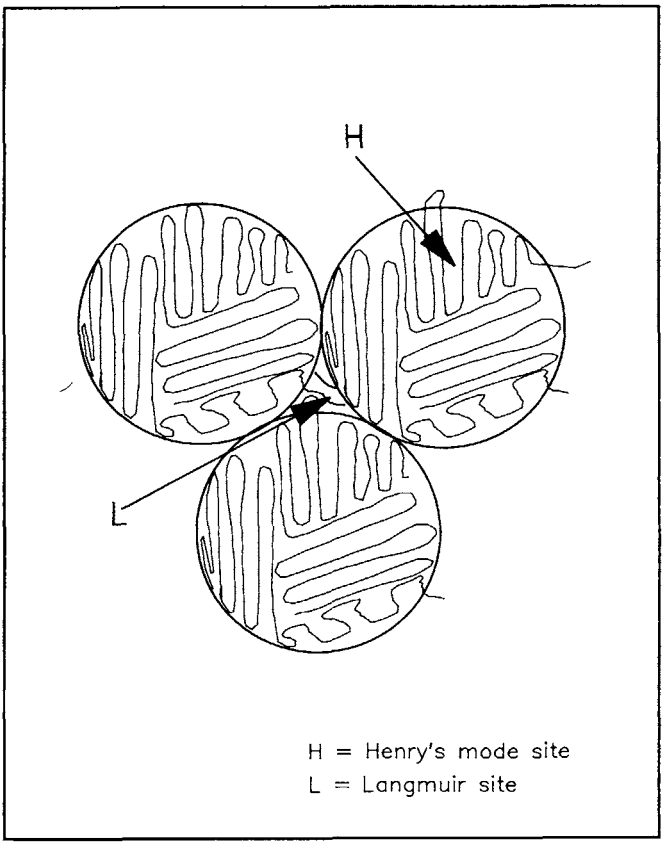


Fig. 1. The intra- and internodular chain displacement/dual-mode model.

that approximates that of thick dense films of the same material. The most effective means of sealing to date involves coating with a permeable polymer such as silicone.[5] The model that is proposed here for dual-mode sorption presupposes a defect-free skin in which displacements between parallel chain segments within and without closely packed glassy nodules represent Henry's mode and Langmuir absorption sites, respectively. This model is specific, graphic, consistent with available physical evidence, and can accommodate changes between intra- and internodular chain segment displacements, which are, to some extent at least, independent of one another.

## Fibers from Sols with Neat Solvent Vehicles

In retrospect, it is clear that the choice of solvents for this study was an important factor in the subsequent discovery and rationalization of trilayer morphology. A variety of polar basic solvents that covered a range of solubility parameters was chosen. Four of these solvents had previously been employed in the preparation of PSU membranes: dimethylformamide (DMF) for ultrafiltration (UF),[21] dimethylacetamide (DMAC) for microfiltration (MF),[22] *N*-methyl pyrrolidone (NMP) for UF,[6] and formyl piperidine (FP) for gas-separation (GS).[23] A fifth solvent, triethyl phosphate (TEP) had not previously been used in the preparation of PSU membranes. It had, however, been shown to prevent curling of the edges in flat-sheet membranes of polyvinylidene fluoride.[24] A relationship between edge curling and shrinkage was suspected by the present authors. Selected properties of solvent, sols, and fibers for the five neat solvents are found in Table II. Solvent strength is generally considered to be inversely related to the difference $\Delta$ between the Hildebrand solubility parameter of the solvent and that of the polymer.[10] On that basis, NMP and DMAC with $\Delta$'s of $\sim 0.5$ $(\text{cal/cc})^{1/2}$ are the strongest solvents for PSU and DMF is the weakest. Although an inverse relationship between $\Delta$ and selectivity was anticipated,[4,11] none was found. Furthermore, with the exception of the FP fibers, the difference between the selectivities of the fibers is not considered significant. The low selectivity for the FP fibers is thought to be an artifact related to the presence of macrovoids.[25] Nor is there any correlation between $\Delta$ and oxygen permeability. *There does, however, appear to be a trend for oxygen permeability to increase with both sol viscosity and solvent molecule size (molar volume)* (Table II, Fig. 2). Sol viscosity is known to be related to solvent viscosity, which, in turn, is a function of the size (and shape) of the solvent molecule. A macromolecule can be considered as a persistent or wormlike chain.[26] The chain is represented by a line in space, the curvature of which depends on the persistence length. The latter determines chain stiffness and viscosity and increases with the cross-sectional area of the solvated chain, which, in turn, is governed by the size and shape of the solvent molecule. This is believed to be the first report of a relationship between solvent molecule size and film gas permeability. The reinterpretation of some earlier results[27] along these lines now appears appropriate. This relationship is significant and suggests that intra- and internodular chain segment displacements are related to the size of the *transient* molecular spacers or templates that sheath the macromolecules in solution. Analogous effects are known for *per-*

TABLE II
Selected Solvent, Sol, and Gel Properties for Fibers Spun from 32% Polysulfone in Neat Solvent Vehicles

| Solvent | $\delta_t$ $(cal/cc)^{1/2}$ | $\Delta^a$ $(cal/cc)^{1/2}$ | Molar volume (cc/mol) | Sol viscosity (cps 30°C) | $O_2$ $P/l$ $(GPU)^b$ | $\alpha_{N_2}^{O_2}$ |
|---|---|---|---|---|---|---|
| Triethyl phosphate (TEP) | 11.2 | 0.65 | 171 | 360,000 | 26.1 | 3.3 |
| Formyl piperidine (FP) | 11.7 | 1.15 | 111 | 201,750 | 10.2 | 2.1 |
| *N*-methyl pyrrolidone (NMP) | 11.0 | 0.45 | 96.5 | 44,000 | 4.4 | 3.0 |
| Dimethyl formamide (DMF) | 12.4 | 1.85 | 77 | 23,650 | 4.3 | 2.9 |
| Dimethyl acetamide (DMAC) | 11.05 | 0.50 | 92.9 | 17,300 | 9.4 | 3.5 |

[a] $\Delta = \delta_t$ solvent $- \delta_t$ Udel PSU; [$\delta_t$ PSU = 10.55 $(cal/cc)^{1/2}$].
[b] GPU = $cm^3/cm^2$ s cm Hg ($\times 10^6$).

*manent* templates in the form of bulky side groups on polymer chains.[28,29] It is, of course, more costly to synthesize a new bulky polymer than to employ bulky solvent molecules. Furthermore, the mechanical properties of a polymer are often adversely affected by the introduction of bulky side chain groups.

A potential problem associated with the use of bulky solvent molecules as templates is their low diffusivity that exacerbates their subsequent extraction. Indeed, the removal of FP (molar volume ~ 110 cc/mol) from the first-generation PSU fiber required extensive washing. Even greater difficulties were encountered in the present study for extraction of TEP (molar volume ~ 170

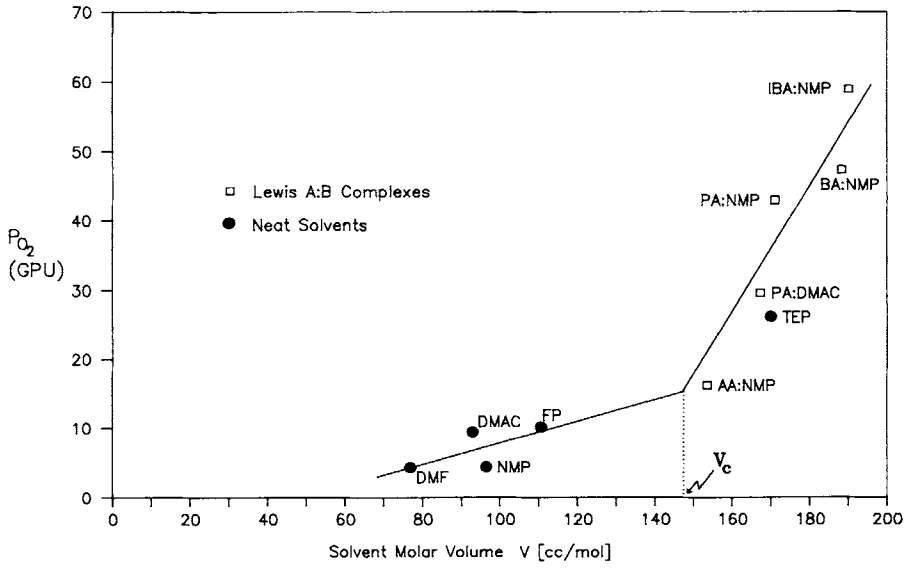


Fig. 2. The relationship between solvent vehicle size and oxygen permeability.

cc/mol). However, the leaching of solvent molecules with molar volumes $\leq \sim 100$ (NMP, DMAC, and DMF) is accomplished much more readily. From this it may be deduced that these exists a critical molar volume $V_c$ for solvents for PSU (and undoubtedly for other polymers as well) that serves as a boundary between solvents with a modest template effect and those with an appreciable template effect. A further problem is associated with slow extraction, namely, plasticization by the retained solvent. In such a case, excess free volume initially frozen into the polymeric glass is lost as a result of densification. In any event, the use of large solvent molecules as templates is fraught with difficulty.

### Fibers from Lewis Acid : Base Complexes as Solvent Vehicles

A possible means of circumventing problems associated with the use of **supra** $V_c$ solvents is to employ vehicles that contain transiently stable complexes [eq. (1)]:

$$A + B \rightleftharpoons A:B \tag{1}$$

where *A* and *B* are nonsolvent and solvent molecules, respectively, and *A* : *B* is an association complex, in which $V_A, V_B < V_c < V_{A:B}$ where $V_A$, $V_B$, and $V_{A:B}$ signify the molar volumes of A, B, and A : B and $V_c$ signifies the critical molar volume.

The stability of *A* : *B* beyond the sol → gel transition is unnecessary and, by analogy to the case of vehicles consisting of neat solvents with $V > V_c$, may even be harmful. Since the fibers are wet-spun, it was decided to employ hydrolytically unstable complexes that would disintegrate into their small easily extractible component parts on contact with water. Hydrogen-bonding complexes consisting of Lewis acids and bases are known. Convenient scales for the measurement of relative strengths of Lewis acids and bases, respectively, are the Gutmann acceptor number (AN) and donor number (DN) series.[8,9] Both series include water and, therefore, permit an estimation of the hydrolytic stability of Lewis acid : base (A : B) complexes. Spectrophotometric evidence for the existence and stability of these complexes has been obtained (Fig. 3, Tables III and IV). Lewis A : B complexes were chosen to further test the solvent template-free volume hypothesis because a large number of such complexes of varying stability can be prepared, because stoichiometric relationships exist that simplify the selection of A : B ratios, and because favorable results were obtained by other workers[5,6] in the use of inorganic acids to increase the permeability of PSU ultrafiltration membranes (Table I). Because the number of Lewis acids and bases is so large and the number of A : B complexes even larger, initial attention was focused on a single basic solvent (B), NMP, not only for aesthetic and environmental reasons, but also because of its use in earlier studies[6] and because the close correspondence between its $\delta_t$ and that of Udel® PSU (Table II) was consistent with the attainment of maximum selectivity.[4,11] The acid (A) components of A : B were usually nonsolvents. However, 2-chloropropionic acid was an exception to this rule.

Sulfuric acid has an AN of 130.1 and is the strongest Lewis acid among those listed (Table III). It was not known whether $H_2SO_4$ would form 1 : 1 or

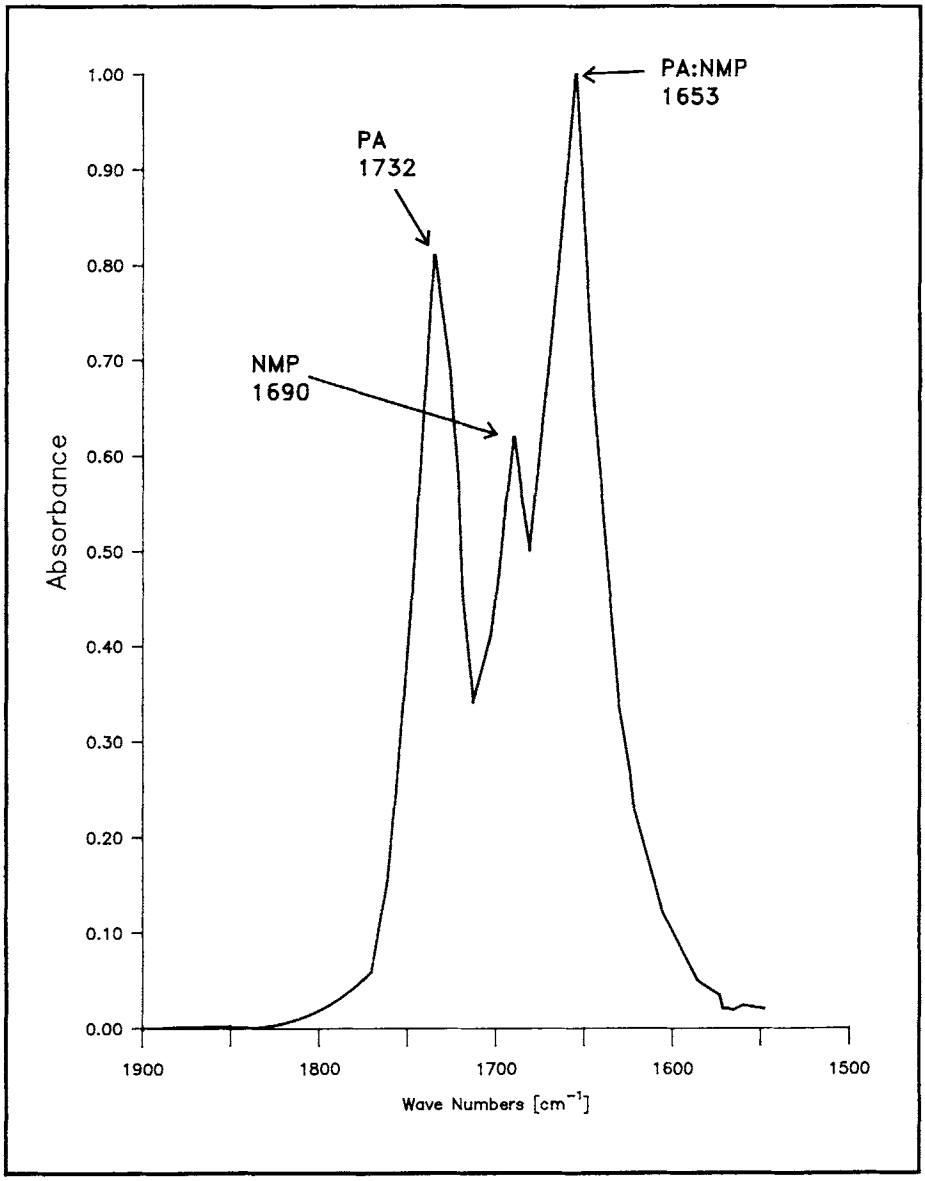


Fig. 3. Infrared spectra of carbonyl bands: PA, NMP, PA : NMP complex.

1 : 2 complexes (or both) with NMP. The addition of 1 mol of $H_2SO_4$ to 1 mol of NMP was accompanied by a strong exotherm, and after cooling resulted in an almost colorless viscous liquid. This complex was stable over a period of at least several months. Polysulfone was insoluble in the neat complex. It was, therefore, necessary to add the complex to an NMP solution of PSU before a sol containing the complex could be spun. The vehicle contained 5% $H_2SO_4$. The result was negative (Table III). Permeability and selectivity were low, and the $T_g$ lay 4–5°C below that of bulk PSU, which suggested the presence of

TABLE III
Lewis Acid AN, $\Delta\nu$(C=O)'s, $T_g^*$'s, and Air Separation Characteristics for Polysulfone Fibers from 37% TS Sols in NMP

| Lewis acid | AN | $\Delta\nu$(C=O) ($cm^{-1}$) | $T_g^*$ [a] (°C) | $O_2$ $P/l$ (GPU)[b] | $\alpha_{N_2}^{O_2}$ |
|---|---|---|---|---|---|
| Formamide | 39.8 | −5 | 185, 186 | 8.3 | 4.7 |
| Ethylene carbonate | 22.3 | 0 | 163, 164 | 4.0 | 2.4 |
| Glycerol | 49.4 | −12 to −16 | 183, 183 | 4.7 | 5.0 |
| Acetic acid (AA) | 52.6, 52.9 | −36 to −38 | 189 | 16.2 | 4.9 |
| Propionic acid (PA) | 49.1 | −36 to −38 | 195 | 43 | 5–5.2 |
| Butyric acid (BA) | 48.3 | −36 to −38 | 195 | 47.4 | 5.0 |
| Isobutyric acid (IBA) | 47 | −36 to −38 | 197 | 58.9 | 2.5 |
| 2-chloropropionic acid (2CP) | 62.4 | −46 | — | 47 | 4.3 |
| Sulfuric acid | 130.1 | — | 185, 186 | 8.5 | 3.5 |

[a] $T_g$ of bulk PSU = 190°C.
[b] GPU = $cm^3/cm^2$ s cm Hg ($\times 10^6$).

residual A : B complex. The apparent stability of this A : B complex in water is believed to be a result of the greater acid strength of $H_2SO_4$ (AN = 130.1) relative to that of water (AN = 54.8). In any event, it was apparent that the $H_2SO_4$ : NMP complex did not represent a sol component that could be effectively used as a transient template to increase free volume.

At this juncture it was decided to focus on organic Lewis acids and, more specifically, on the $C_1$–$C_4$ monocarboxylic acids. For purely aesthetic reasons, propionic acid (PA) was chosen as the first Lewis acid. The choice of PA rather than acetic acid AA was fortuitous, because the permeability of the fibers spun from AA : NMP was only marginally greater than that of the first-generation fiber that was spun from formamide : formyl piperidine (Figs. 2 and 4). The results were highly salubrious. They not only supported the transient template-free volume hypothesis but led immediately to an eminently successful program

TABLE IV
Selected Properties of Lewis A : B Complexes vs. Air-Separation Characteristics of Polysulfone Fibers Spun from 37% TS Sols

| Complex[a] | DN | A : B (% w/w) | $\Delta\nu$(C=O) ($cm^{-1}$) | $\delta_V$[b] $(cal/cc)^{1/2}$ | $\Delta$[c] $(cal/cc)^{1/2}$ | $O_2$ $P/l$ (GPU)[d] | $\alpha_{N_2}^{O_2}$ |
|---|---|---|---|---|---|---|---|
| PA : DMAC | 27.8 | 30/37 | −31 | 11.09 | 0.54 | 29.6 | 4.8 |
| PA : NMP | 27.3 | 43/57 | −36 to −38 | 11.63 | 1.08 | 43 | 5–5.2 |
| AA : NMP | 27.3 | 38/62 | −36 to −38 | 11.45 | 0.90 | 16.2 | 4.9 |
| PA : FP | 27 | 38/62 | −32 to −33 | 11.75 | 1.20 | 24.7 | 5.2 |
| PA : DMSO | 29.8 | 7/93 | −37 | 12.17 | 1.62 | 9.0 | 5.2 |
| PA : DMF | 26.6 | 25/75 | −25 to −26 | 12.04 | 1.49 | 26.2 | 3.7 |

[a] PA = propionic; AA = acetic acid.
[b] $\delta_V = \delta_t$ vehicle.
[c] $\Delta = \delta_t$ vehicle − $\delta_t$ Udel PSU; [$\delta_t$ PSU = 10.55 $(cal/cc)^{1/2}$].
[d] GPU = $cm^3/cm^2$ s cm Hg ($\times 10^6$).

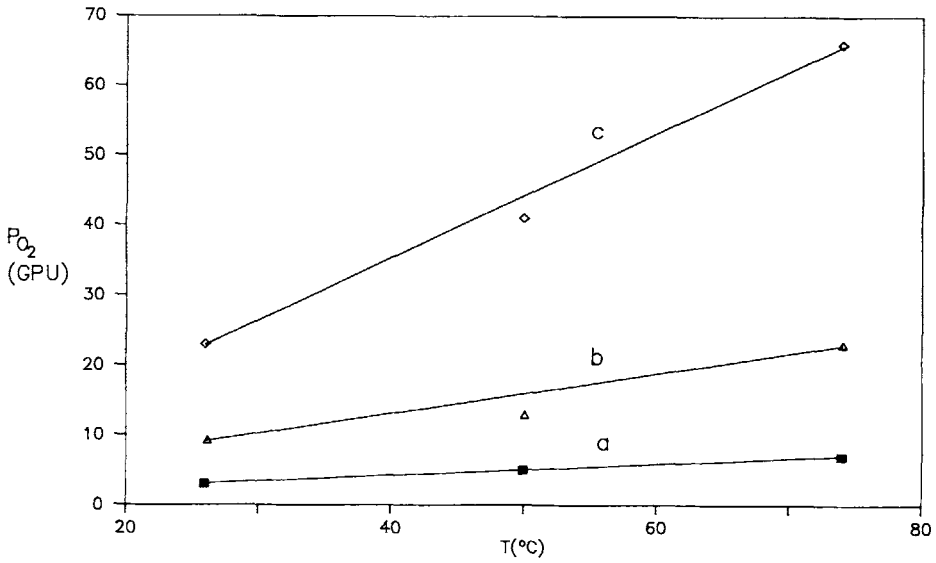


Fig. 4. Oxygen permeation vs. temperature for PSU fibers spun from sols with various vehicles: (a) NMP, (b) formamide-FP, (c) PA : NMP.

to study, develop, and commercialize the second-generation PSU gas-separation membrane.[7] Permeability increases with increasing $\mathbf{V}_{A:B}$. The increase in $O_2$ $P/l$ with $\mathbf{V}$ is modest up to $\mathbf{V}_c \sim 147$ cc/mol. This value was taken as the intersection of the extrapolated linear curves corresponding to low slope and high slope ranges (Fig. 2). Above $\mathbf{V}_c$, the curve rises steeply, but selectivity is maintained to a $\mathbf{V}$ of $\sim 188$ cc/mol. At a $\mathbf{V}$ of 190 cc/mol, selectivity declines precipitously (Table III).

## Nature of Lewis A : B Complexes

A Lewis acid A is an electron-pair acceptor, and a Lewis base B an electron-pair donor. The prototype of B in this instance is NMP, the resonance forms for which are[30]

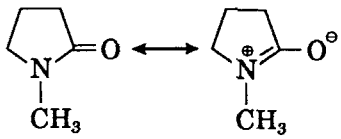

The prototype of A is propionic acid PA. For PA : NMP, the complex that is given generically as A : B in eq. (1) takes the specific form depicted in eq. (2):

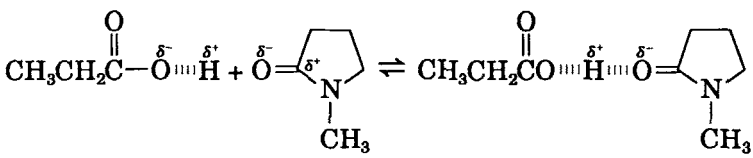

(2)

Spectrophotometric evidence for the existence of the PA : NMP complex is presented in Figure 3. A measure of the strength of the A : B complex is $\Delta\nu$, the observed shift in $cm^{-1}$ of the C=O band frequency in the IR spectrum of pure NMP. In the case of FP, DMAC, and DMF, the amidic C=O band, and in the case of DMSO, the S=O band, is monitored. For purposes of this discussion, an effective A : B complex is one that yields fibers with $O_2$ permeabilities (GPU) greater than $\sim$ 10 with selectivities $\geq \sim$ 5 (13.6 atm at 50°C). These conditions are encountered for complexes with $\sim 30 < \Delta\nu < \sim 40$, that is, for PA : DMAC, PA : NMP, AA : NMP, and PA : FP (Table IV). These are complexes that in addition to having sufficient stability and a $\mathbf{V} > \mathbf{V}_c$, are sufficiently strong solvents (as indicated by a $\Delta < \sim 1.3$ $(cal/cc)^{1/2}$. The complexes PA : DMSO and PA : DMF with $\Delta\nu$'s within or close to the desired stability range are nevertheless ineffective because of inadequate solvent power ($\Delta > 1.3$ $[cal/cc]^{1/2}$). Lewis acids such as 2-chloropropionic acid and sulfuric acid form complexes that are too strong and, hence, too stable to hydrolysis to undergo rapid disassociation and leaching on gelation in water. Other Lewis acids such as formamide, ethylene carbonate, and glycerol (Table III) do not form complexes of sufficient stability to permit their serving as effective transient templates. The most effective A's and B's are those with $41 < AN < 53$ (Table III) and $27 < DN < 28$ (Table IV), respectively.

Since an equilibrium exists between A : B and unassociated A and B, the effective molar volumes of solvent vehicles containing A : B will be lower than are the calculated values presented in Figure 2. For the same reason, the effective molar volumes of solvent vehicles in which the molar A : B ratio < 1 will be still lower. An important consequence of this is that the template spacer effect of A : B will be diminished or absent altogether at low A : B ratios. Evidence for this is the increase in permeability with increasing A : B ratio up to and slightly beyond unity (Table V). The one anomalously high permeability (membrane 1) is believed to be a result of unsealable defects in the skin as indicated by its low selectivity.[25]

### The Relationship between Permeability, First-heat Glass Transition Temperature, and Free Volume

The model that has been presented here to explain the higher permeability at constant selectivity assumes a skin whose surface defects have been sealed by a highly permeable polymer.[1] According to our model, increased permeability in the second-generation membrane is a result of decreased macromolecular packing density within and between the nodules in the glassy skin. Density can also be expressed in terms of its reciprocal, namely, the specific volume. We are, of course, not interested in the total specific volume that includes that fraction occupied by the polymer chains, but only in that fraction of the specific volume that is available for gas transport, or in other words, the free volume. Free volume is a three-dimensional concept that is analogous to interchain displacement in a single dimension.[11] Because of the presence of excess free volume, the enthalpies of the second-generation PSU membranes are greater than those of, for example, bulk polymer or melt-extruded films. As a result, the first-heat glass transition temperatures, $T_g^*$'s, of fibers spun from sols containing vehicles with A : B complexes $> \mathbf{V}_c$ are higher than $T_g^*$'s of fibers spun

TABLE V
Effects of Propionic Acid Concentration in 37% Polysulfone/NMP Sols on Fiber Properties

| Membrane no. | PA/NMP | | $T_g^*$ (°C) | $O_2$ $P/l$ (GPU)[a] | $\alpha_{N_2}^{O_2}$ |
|---|---|---|---|---|---|
| | Molar | % w/w | | | |
| 1 | 1.09 | 45/55 | 197 | 45.9 | 4.6 |
| 2 | 1.00 | 43/57 | 195 | 43 | 5–5.2 |
| 3 | 0.89 | 40/60 | 197 | 33 | 4.4 |
| 4 | 0.72 | 35/65 | 197 | 25 | 4.8 |
| 5 | 0.57 | 30/70 | 197 | — | — |
| 6 | 0.42 | 26/74 | 187 | 16.3 | 4.3 |
| 7 | 0.33 | 20/80 | 187 | 29.6 | 2.6 |

[a] GPU = $cm^3/cm^2$ s cm Hg ($\times 10^6$).

from sols containing vehicles that do not exert a template-spacer effect (Tables III, V, and VI). It should be realized that once a glass has been subjected to an initial excursion through the $T_g$ range, free volume and enthalpy will have decreased, so that subsequent excursions (or heats) will only yield the lower $T_g$ that is characteristic of the bulk material. Since the standard differential scanning calorimetry (DSC) procedure is to cycle a sample through the $T_g$ range until a constant $T_g$ is obtained, higher initial values are typically not recorded. It was only because we deliberately set out to use DSC to explore the glassy state that we became what we believe to be the first membranologists to encounter and explain this phenomenon in terms of its effect on gas permeability! The basic principles involved have long been taught by polymer glassy-state physicists.[31–33] The relationship between $T_g^*$, now a valid surrogate for relative free volume, and permeability can be found in Tables III, V, and VI.

The maintenance of "intrinsic" selectivity in conjunction with a fourfold increase in permeability (Fig. 4) requires an explanation since permeability

TABLE VI
Lewis A : B Complex Status vs. $T_g^*$'s and Air-Separation Characteristics of Fibers from Aromatic Sulfone Polymers

| Polymer | Class | TS (%, w/w) | Lewis acid | A : B complex status (yes or no) | $O_2$ $P/l$ (GPU)[a] | $\alpha_{N_2}^{O_2}$ | $T_g^*$ |
|---|---|---|---|---|---|---|---|
| Udel 2500 | PSU | 3 | Formamide[b] | No | 8.3 | 4.7 | 185 |
| Udel 3500 | PSU | 37 | PA[c] | Yes | 43 | 5–5.2 | 195 |
| Victrex 600 | PES | 40 | Formamide[b] | No | 2.3 | 3.4 | 218 |
| Victrex 600 | PES | 40 | PA[c] | Yes | 13.1 | 5.1 | 235 |
| Radel A400 | PPS | 37 | Formamide[b] | No | 6.2 | 5.2 | 221 |
| Radel A400 | PPS | 37 | PA[c] | Yes | 20 | 4.4 | 232 |

[a] GPU = $cm^3/cm^2 \cdot s \cdot cmHg$ ($\times 10^6$).
[b] Formamide 13/NMP 87 (% w/w).
[c] PA 43/NMP 57 (% w/w).

and selectivity in dense films are generally considered to be coupled. The explanation lies in the asymmetry of the membrane skin. This was established by etching with oxygen plasma the skins of first- and second-generation PSU membranes. The selectivity of the two sets of membranes as a function of the time of exposure to oxygen plasma was then measured (Fig. 5). The selectivity of the first-generation membrane remained unchanged up to etch periods of 1 min, whereas the selectivity of the second-generation membrane underwent an immediate decline. This suggests that the first-generation membrane has a

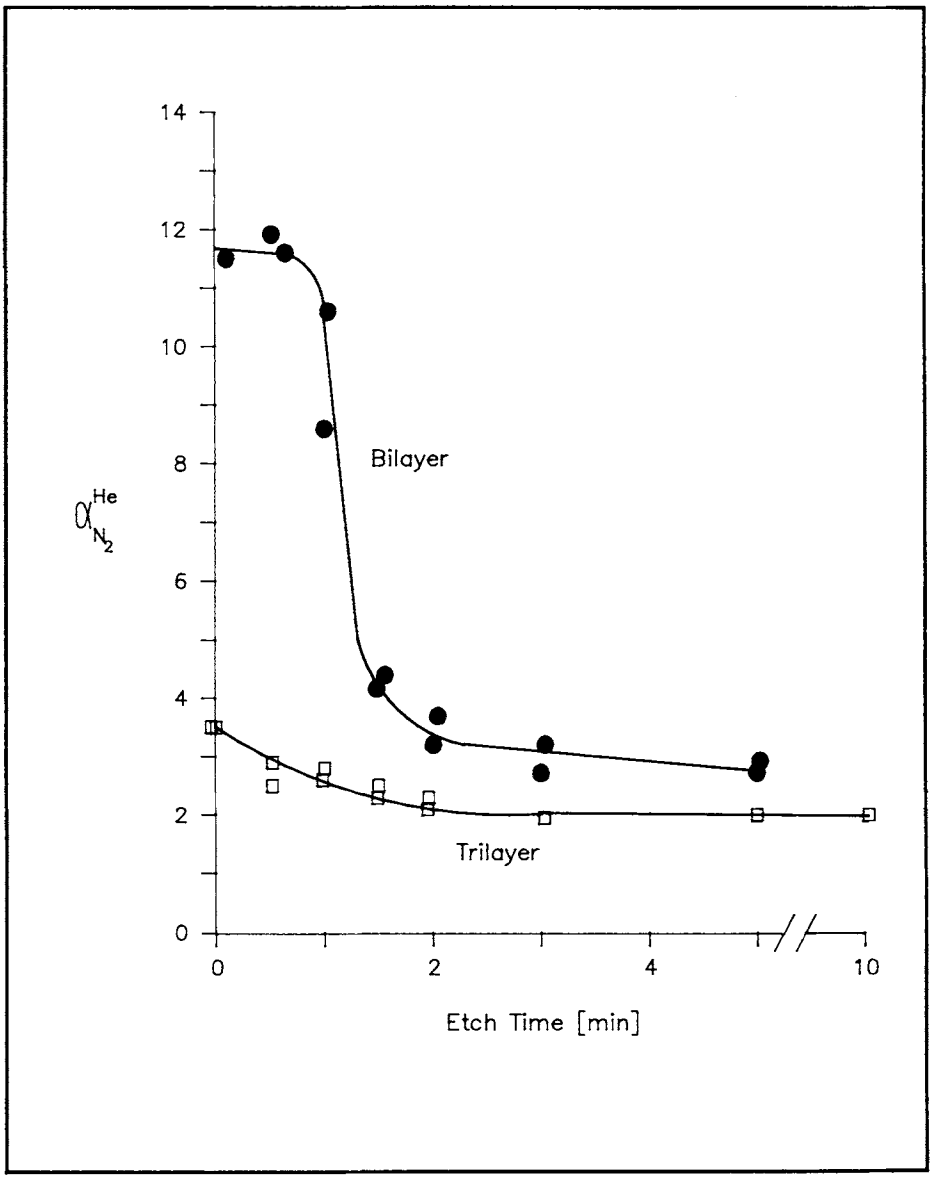


Fig. 5. Separation factors of PSU fibers vs. oxygen plasma etch time: (a) bilayer, (b) trilayer.

relatively thick skin of uniform density, whereas the second-generation membrane exhibits a skin with graded density. Therefore, the first-generation gas-separation membranes can be represented by a *bilayer* composed of a porous substructure surmounted by a uniform density skin. The second-generation membrane, on the other hand, can be considered as a *trilayer* consisting of a porous substructure that supports a skin that is further divided into two layers: an extremely thin active layer and the remainder of the skin (Fig. 6).

The preparation of trilayer membranes by the use of Lewis A : B complexes as transient templates is by no means restricted to membranes from Udel® PSU (Table VI). It appears to be generally applicable to hydrophobic polymers.[7] Approximately fivefold increases in permeability with no loss in selectivity appear to be the norm.

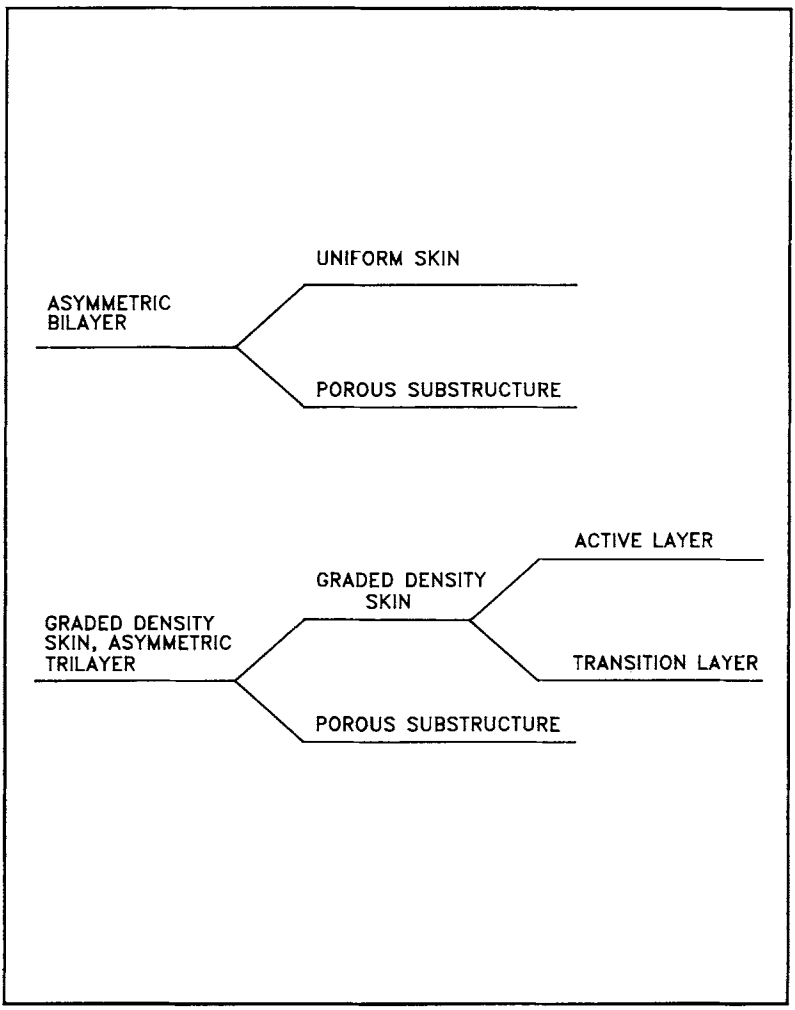


Fig. 6. Schematic representation of an asymmetric bilayer and a graded density skin asymmetric trilayer.

## CONCLUSIONS

1. A second-generation PSU gas-separation membrane has been developed. This membrane exhibits a fourfold increase in $O_2$ permeability at constant $O_2/N_2$ selectivity when compared to the first-generation membrane.
2. The difference in gas-separation characteristics between first- and second-generation membranes is due solely to differences in physical structure, specifically to increased free volume and anisotropy in the skin of the latter. Direct physical evidence for increased free volume is the elevated first-heat glass-transition temperature, $T_g^*$. Direct evidence for the graded density skin is the immediate decline of selectivity with oxygen plasma etching time in the second-generation membrane. In contrast, the first-generation membrane exhibits a uniform density skin as shown by the maintenance of a selectivity plateau before the onset of a selectivity decline.
3. A relationship is apparent between solvent molecule size and the free volume and permeability of the resultant membranes. A critical solvent molar volume, $V_c$, exists ($\sim$ 147 cc/mol for PSU), in excess of which substantial increases in free volume and permeability result.
4. Lewis acid : base complexes (A : B) are used as transient templates to control free volume and permeability in the second-generation PSU membrane. Unlike a large neat solvent with its low diffusivity, an A : B can be easily removed because it is hydrolytically unstable and disintegrates on contact with water into its small easily extracted component parts. Optimum stability in A : B is obtained by acids with Gutmann 47 $<$ AN $<$ 53 and bases with 27 $<$ DN $<$ 28.
5. Selectivity is maximized by the use of sols with $\Delta$'s $(\delta_{A:B} - \delta_{PSU}) < 1.3$ $(cal/cc)^{1/2}$.

## References


1. J. S. Henis and M. K. Tripodi, U.S. Patent 4,230,463.
2. S. Loeb and S. Sourirajan, U.S. Patent 3,133,132.
3. M. Panar, H. Hoehn, and R. Hebert, *Macromolecules*, **6**, 777 (1973).
4. R. E. Kesting, *Synthetic Polymeric Membranes: A Structural Perspective*, 2nd Ed., Wiley-Interscience, New York, 1985.
5. I. Cabasso, E. Klein, and J. K. Smith, P'B-248 666, 1975.
6. T. Tweddle, O. Kutowy, W. Thayer, and S. Sourirajan, *Ind. Eng. Chem., Prod. Res. Dev.*, **22**, 320 (1983).
7. R. Kesting, A. Fritzsche, M. Murphy, C. Cruse, A. Handermann, and R. Malon, U.S. Pats. 4,871,494 and 4,880,441.
8. V. Gutmann et al., *Monats. Chem.*, **106**, 1235 (1975).
9. K. Mayer, *Pure Appl. Chem.*, 1697, (1979).
10. A. Barton, *CRC Handbook of Solubility Parameters and Other Cohesion Parameters*, CRC Press, Boca Raton, FL, 1983.
11. R. E. Kesting, *The Nature of Pores in Integrally-skinned Phase Inversion Membranes*, paper presented at 195 American Chemical Society Meeting, Toronto, June 7, 1988.
12. A. G. Wonders and D. R. Paul, *J. Membrane Sci.*, **2**, 63 (1979).
13. A. Chan and D. R. Paul, *J. Appl. Polym. Sci.*, **24**, 1539 (1979).
14. R. E. Robertson, *J. Polym. Sci., Symp.*, **63**, 173 (1978).
15. R. Pace and A. Datyner, *Polym. Eng. Sci.*, **20**(1), 51 (1980).

16. S. Sourirajan and T. Matsuura, *Reverse Osmosis and Ultrafiltration: Science and Principles,* Nat. Res. Council Canada, Publ. 24188, 1985.

17. R. E. Kesting, *J. Appl. Polym. Sci.,* **17,** 1771 (1973).

18. R. Schultz and S. Asunmaa, *Rec. Prog. Surf. Sci.,* **3,** 291 (1970).

19. K. Kamide and S. Manabe, in *Materials Science of Synthetic Membranes,* D. Lloyd, Ed., Am. Chem. Soc. Symp. Series 269, American Chemical Society, Washington, DC, 1985.

20. A. K. Fritzsche et al. *J. Appl. Polym. Sci.,* (1990).

21. A. S. Michaels, U.S. Patent 3,615,024.

22. I. Cabasso, E. Klein, and J. K. Smith, *J. Appl. Polym. Sci.,* **20,** 2377 (1976).

23. E. Brooks et al., U.S. Patent 4,364,759.

24. W. Benzinger, U.S. Patent 4,384,041.

25. R. E. Kesting, A. K. Fritzsche, M. K. Murphy, C. A. Cruse, A. C. Handermann, R. F. Malon, and M. D. Moore, *J. Appl. Polym. Sci.,* **40,** 1575 (1990).

26. G. Porod, *Monats. Chem.,* **80,** 251 (1949).

27. R. Roberts and K. Kammermeyer, *J. Appl. Polym. Sci.,* **1,** 2183 (1963).

28. R. T. Chern, W. T. Koros, H. P. Hopfenberg, and V. T. Stannett, in *Materials Science of Synthetic Membranes,* Am. Chem. Soc. Symp. Series 269, American Chemical Society, Washington, DC, 1985.

29. N. Muruganandam and D. R. Paul, *J. Membr. Sci.,* **34,** 185 (1987).

30. Anon., NMP, N-methyl-2-pyrrolidone, GAF Corp. 1972.

31. L. C. E. Struik, *Physical Aging in Amorphous Polymers and Other Materials,* Elsevier, New York, 1978.

32. M. R. Tant and G. L. Wilks, *Polym. Eng. Sci.,* **21**(14), 874 (1981).

33. S. Matsuoka, *Polym. Eng. Sci.,* **21**(14), 970 (1981).

Received November 28, 1988
Accepted August 17, 1989